The Photorefractive Effect: A Study in Non-Linear Optics

Theodore Rogozinski
Performed In Collaboration with Alexander Strang
Department of Physics, Case Western Reserve University
Cleveland, OH
(Dated: April 1, 2016)

The behavior of light can change drastically depending on its medium. In non-linear materials such as the $Bi_{12}SiO_{20}$ (BSO) crystal used in this experiment, light can change it's intensity based on whether another, independent light beam is crossing it within the crystal. This coupling of the beams is known as The Photorefractive Effect. To study this effect, this experiment utilized 2 techniques: 2-beam coupling and 4-wave mixing. The 2-beam coupling produced a clear, measurable effect which, rather unfortunately, could not be analyzed fully due to missing coefficients which were unobtainable in the time frame allowed. The 4-wave mixing yielded no correlation at all. After an initial failure to get an effect from the 4-wave mixing, considerable effort was directed towards re-configuring the experiment with no results. In addition to this, when a high voltage was put across the crystal, no conclusive increase in the mobility of the charge carriers was observed. Most likely due to the naturally quick response of the crystal with no induced electric field.

I. INTRODUCTION

Discovered in the 1980's, The Photorefractive Effect was found on accident as a source of error and was thought by its discoverers to be "Highly detrimental to the optics of nonlinear devices based on these crystals." After almost 40 years of relatively intense study, The Photorefractive Effect remains one of the best prospects for applications like holograms and phase conjugation.

In this experiment 2 methods were used to observe The Photorefractive Effect: 2-Beam Coupling and 4-Wave Mixing. Both of them were designed to induce the effect using 2 beams crossing in a crystal, thus moving the charge carriers within them to change the overall refractive index. (Explained more carefully in II) 2-Beam Coupling was designed to be a light introduction while the 4-Wave Mixing was meant to reduce error and possibly measure the time delay associated with the effect.

It should be mentioned that for the 2-Beam Coupling a so-called "eletro-optic coefficient" was needed in order to calculate the exact prediction. The equation that this coefficient would be used in can be found in [1] and is given by

$$\Delta n = -\frac{n^3 r}{2} E_{sc} \propto r_e \sin\left(\frac{2\pi x}{\Lambda}\right). \tag{1}$$

Where r_e is the electro-otpic coefficient, E_{sc} is the electric field across the crystal, and Δn is the change in the refractive index due to The Photorefractive Effect. Other parameters will be explained in more detail in II. Without the electro-otpic coefficient, it is impossible to make any direct predictions concerning the photorefractive effect of a material. While the coefficient could have been measured while data for the 2-Beam coupling was taken, it was unfortunately forgotten.

II. THEORY

All of the content in the theory section can be found in [1]. The reader is encouraged to read [1] for a more complete understanding of the theory involved in the experiment.

The Photorefractive Effect is a combination of photoconductivity and the electro-optic effect. In the photorefractive material there are donor impurities and acceptor impurities. With no applied electric field or incident beams to excite the charge carriers, (electrons in this experiment) they simply sit in the crystal with an approximately even distribution. After they are excited, the charge carriers drift into regions of the crystal where there is less light. These abnormalities in the charge of the crystal produce electric fields within it which can modify the incident light beams.

Taking this simple "Band Transport Model" The Photorefractive Effect can be broken down into 4 major phases. In the words of [1] they are "photogeneration of charge carriers, transport of mobile carriers, trapping of these carriers, and change of refractive index."

The experiment begins with 2 light beams labeled by

$$\mathcal{E}_1 = \tilde{\mathcal{E}}_{10} e^{i\phi_1} e^{-i\vec{k_1}\vec{r}} \text{ and } \mathcal{E}_2 = \tilde{\mathcal{E}}_{20} e^{i\phi_2} e^{-i\vec{k_2}\vec{r}}. \tag{2}$$

Where ϕ_1 and ϕ_2 are their phases, a radius vector $\vec{r}$, and wave vectors $\vec{k_1}$ and $\vec{k_2}$. We read the intensity of the light as

$$I_{tot} = |\mathcal{E}_1 + \mathcal{E}_2|^2 = \mathcal{E}_{1_0}^2 + \mathcal{E}_{2_0}^2 + 2\mathcal{E}_{1_0}\mathcal{E}_{2_0}\cos(\vec{K}\vec{r} + \phi_1 - \phi_2). \tag{3}$$

Where $\vec{K} = \vec{k_1} - \vec{k_2}$ is the grating vector. This interference pattern has a spacial wavelength of

$$\Lambda = \frac{\lambda}{2n\sin\tilde{\theta}}. \tag{4}$$

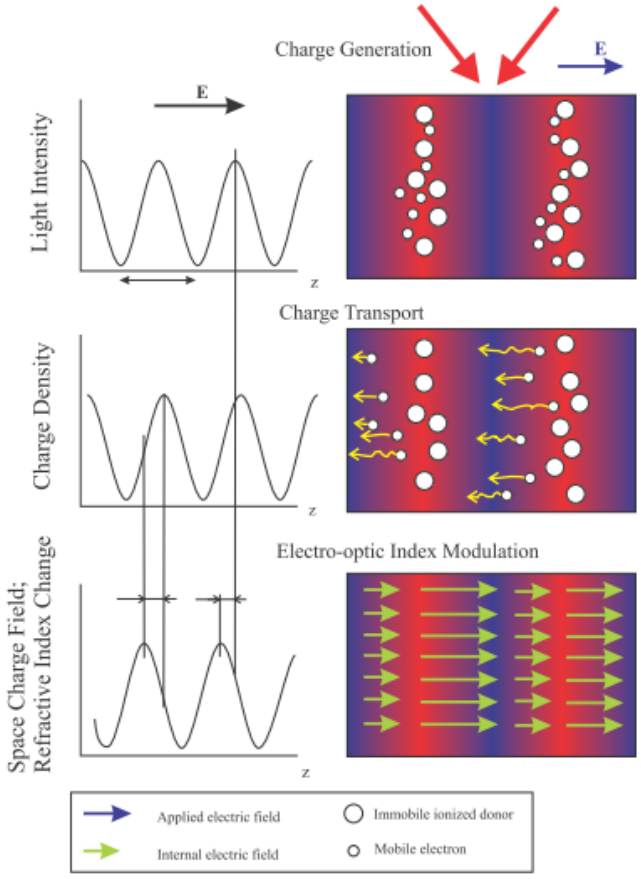

Figure 1: Phases of The Photorefractive Effect. The z axis in the graphs represents distance in the crystal. As the light hits the crystal (top right) the charge carriers move (middle right) and the electric field is created (bottom right).

Please refer to the 3 sections of Fig. 1 for pictures and explanations of next 3 paragraphs respectively.

The photoconductivity of the material turns the energy of the incident light into the the generation of mobile charge carriers.

Next, the charge carriers drift within the crystal because they are no longer bound by atomic forces and can now effectively act on one another. These charge anisotropies in the crystal are often referred to as "charge density gradients." This creates the diffraction grating in the crystal responsible for the phase shifts the outgoing beam by a factor $0 < \phi < \frac{\pi}{2}$.

This rearranging of charge carriers produces an electric field E_{sc} since the distribution of charges is no longer uniform. This induced electric field will be sinusoidal and shifted by a factor of $\frac{\pi}{2}$ from the charge density because of Poisson's Equation:

$$\nabla E_{sc} = \frac{e}{\epsilon_0 \epsilon} \rho. \tag{5}$$

Finally, this electric field distorts the refractive index of crystal proportionally described via Eqn. 1.

The maximum of E_{sc} or the "saturation field" can be quickly reasoned out based on how many charge carriers can move and is described by

$$E_q = \frac{eN_A}{\epsilon_0 \epsilon K}. \tag{6}$$

Where N_A is the number density of acceptor impurities and the rest are simply permittivity coefficients and e is the charge of the electron.

A. 2-Beam Coupling

We wish to solve the wave equation

$$\nabla^2 \mathcal{E} = \mu \epsilon_0 \epsilon \frac{\partial^2 \mathcal{E}}{\partial t^2} \tag{7}$$

for a specially modulated electric field described by $\epsilon = \epsilon^0 + \Delta\epsilon$ determined by

$$\Delta\epsilon = -\epsilon^2 r_e E_{sc}. \tag{8}$$

Because both incident beams are the same frequency and are plane waves, we can eliminate the time dependence by simply putting $-\omega^2$ wherever any 2^{nd} order time derivatives are. Because the beam amplitudes are varying slowly we can reduce the equations to a single variable x. We must also keep in mind that $I_1 = |\mathcal{E}_1|^2$ for when we wish to evaluate our intensities.

Taking these things into account we may reach the equations

$$\frac{dI_1}{dx} + \Gamma \frac{I_1 I_2}{I_1 + I_2} \sin\phi = 0 \tag{9}$$

and

$$\frac{dI_2}{dx} + \Gamma \frac{I_1 I_2}{I_1 + I_2} \sin\phi = 0. \tag{10}$$

Where we have introduced the coupling constant

$$\Gamma = \frac{k_0 n^3 r_e |E_w|}{\cos\tilde{\theta}}. \tag{11}$$

Where the different I's are the intensities of the beams after interacting in the crystal, $k_0 = \omega/c$ is the wave vector in a vacuum, n is the refractive index, E_w is the space-charge field amplitude, and $\tilde{\theta}$ is the internal angle of incidence with the crystal which can be derived from Snell's law.

One may integrate Eqns. 9 and 10 to get that

$$I_1 = \frac{\beta(I_1 + I_2)}{\beta + e^{\tilde{\Gamma} x}} \tag{12}$$

and

$$I_2 = \frac{I_1 + I_2}{1 + \beta e^{\tilde{\Gamma} x}}. \tag{13}$$

where the gain coefficient $\tilde{\Gamma} = \Gamma \sin\phi$ and β is the ratio of the intensity of non-interacting beams I_{1_0}/I_{2_0} (i.e. 1 beam passing through the crystal at a time).

We can manipulate the gain coefficient to get the expression

$$\tilde{\Gamma} = -\frac{1}{\tilde{d}} \ln\left[\frac{I_1}{I_2}\frac{I_{2_0}}{I_{1_0}}\right]. \tag{14}$$

Where

$$\tilde{d} = \frac{d}{\cos(\tilde{\theta})} \tag{15}$$

is the effective thickness of the crystal.

B. 4-Wave Mixing

Because of the lack of effect in the 4-wave mixing only an outline of the proposed calculations will be provided. For a complete description of the 4-Wave Mixing system see [1]

The basic idea for the manipulations in the 4-Wave Mixing was to define an efficiency parameter $\eta = \frac{I_4}{I_3}$ where I_3 is the diffracted beam. It would be found that the parameter will have the relation

$$\eta = \eta_0 e^{-2\nu_{decay} t}. \tag{16}$$

We would then use this equation to fit the value of ν_{decay} in an attempt to quantify the decay of the effect.

III. METHODS

Both of these procedures were performed with a HeNe laser. We noted that the laser takes about 10 minutes to warm up and made sure that the beam was constant.

Lockin amplifiers and a beam chopper were used to decrease noise. The beams that were being measured were sent through a beam chopper at a frequency around 1900 Hz and then amplified by the lockin to reduce noise from ambient light. It was noted that higher chopping frequencies produced less intense beams. However, this should not hinder results since the offset was constant.

Experiments were performed in 2 stages. In the first, data was taken using only the crystal(described in detail in III A and III B). In the second phase an electric field of $\approx$ 5000V was run across 2 parallel plates surrounding the crystal in an attempt to increase the mobility of the charge carriers.

A 1 cm$\times$ 1 cm $\times$ 1 cm $Bi_{12}SiO_{20}$ crystal was used in collecting data. The crystal was bought new for the experiment so it is unlikely that imperfections in the crystal contributed significantly to error.

Components were secured into a pneumatic table in the appropriate configuration using screws. Lights were turned off to reduce noise. Chopper was connected directly to the Lockin in order to ensure accuracy of the measured frequency. Beams were aligned to cross as soon as they hit the crystal.

Lockins and arduino were connected to a computer using 1EEE-48 GPIB with usb connection. Data was taken and shudder was controlled using using MATLAB and graphed in real-time with intervals of approximately a millisecond.

Polarization rotator was set to the plane of incidence with the crystal.

A. 2-Beam Coupling

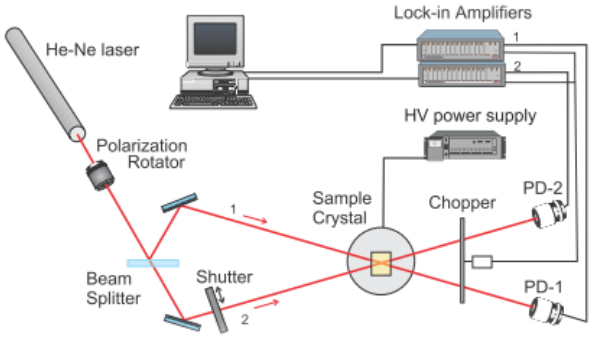

Figure 2: A Schematic diagram for 2-Beam Coupling. The beams cross in the sample crystal, moving the charge carriers to induce an electric field which modifies the intensity of the incident beams.

The table was aligned as in Fig. 2 with the angle between the 2 beams being 14 $\pm$ 1 degree. It was observed that the beam splitters did not evenly split the incident beam.The intensities of the measured beams were around $\frac{1}{3}$ and $\frac{2}{3}$ of the original intensity.

On the day that data was taken a very long power-up time for the laser was allowed ($\approx$20 mins.) to ensure that there would be no skewing due to the laser's warm up period. After this, the shudder was programmed to let the appropriate beam through for 15 seconds and to obstruct it totally for 15 seconds repeatedly. Data was taken over the course of 10 minutes while the shutter was allowed to alternate. Averages for all states of the shutter were found by sampling the peaks and troughs of the graph. After that, one beam shuttered the entire time while the other beam was allowed to pass though the crystal and into the photodiode. This was repeated

again only exchanging which beam was shuttered and which one was allowed to pass through.

About 2 weeks after seeing the effect and taking data we realized that we had forgotten to record the information on the gain coefficient of the crystal. We set up the lab again and took data for different polarizations of the light at an angle of incidence of 22.5°. However on the day that we took this data, we could not reproduce The Photorefractive Effect from before.

B. 4-Wave Mixing

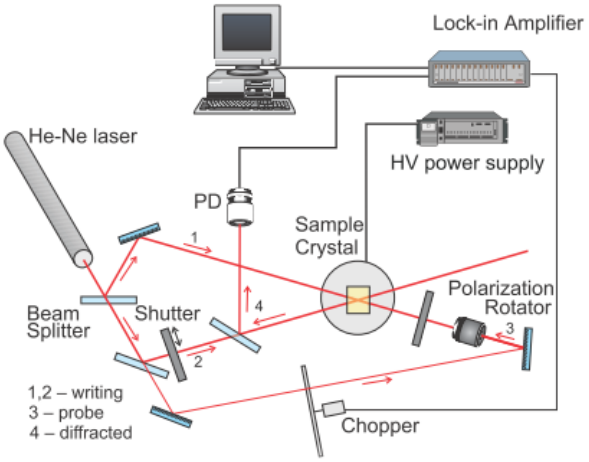

Figure 3: A Schematic diagram for 4-Wave Mixing. Note the non-trivial path of beam 4. The beams cross in the sample crystal, moving the charge carriers to induce an electric field which modifies the intensity of the incident beams

The first Attempt at 4-way mixing was much done in much the same way as III A only making the changes in the setup required in Fig. 3. We were not sure where the correct beam was for the photodiode. There were many unplanned "stray beams" that came from the beam splitters. So we picked the one that looked the most like the angle from Fig. 3.

Laser was allowed a sufficient warm-up time before starting the experiment and lights were turned off to reduce possible error. The lasers hit the crystal at 14°± 1° and the crystal was shuttered for alternating periods of 15 seconds.

C. Corrections to 4-wave Mixing

All of the stray beams were checked to make sure that the one with the effect hadn't simply been missed. Unfortunately, no beams with the effect were found.

After getting no signal from the regular schematic, the beam splitters for 2-way silver mirrors. This was an attempt to see a signal possibly lost by the beam splitters. After this, an "unchopped beam" was measured to see if we could replicate the static obtained when 4-Wave Mixing was first attempted. Lastly, we moved the photodiode around the room and tried to see if any of the stray beams coming from the 2-way silver mirrors. This, again, produced no effect whatsoever when put under rigorous testing.

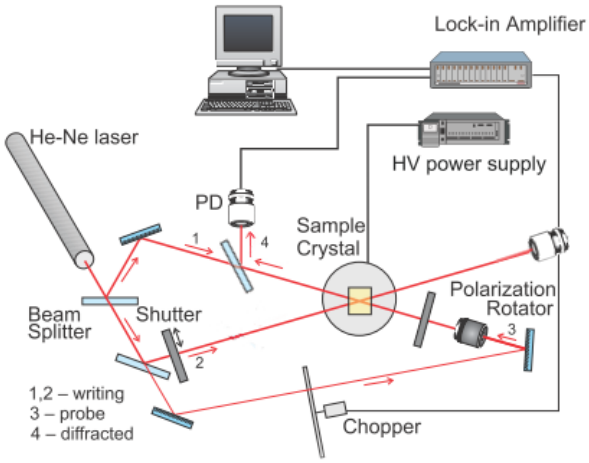

Figure 4: A Schematic diagram for 4-Wave Mixing revised so that the beams may still cross in the crystal, yet the beam heading to photodiode is also the one which passes through the chopper. If one looks back at Fig. 3 one will quickly see that the beam being measured is not the one that has been chopped, thus leaving the experiment vulnerable to errors due to ambient lighting.

By the end, all plausible stray beams were accounted for at a range angles and we still saw no effect that held up to rigorous data analysis.

Moved on to the setup described in Fig. 4. Angle with the crystal was, again, 14°±1°. Again, no effect was observed that held up to rigorous analysis.

IV. RESULTS

All of the data collected in this experiment was given not in terms of intensity, but in terms of the voltage given off by the photodiodes. This is not a problem because if we consider the intensity to be linearly proportional to the voltage output, then we get that

$$\frac{gI_0}{gI_1} = \frac{V_0}{V_1}. \tag{17}$$

Thus it is fine to consider voltage equivalent to intensity so long as we only consider the ratio of any 2 of these intensities.

Table I: The average intensities of the beams measured in volts measured at the peaks and troughs of the graph (see Fig. 8 and Fig.9). Note the decrease in intensity when the 2 beams interact due to the photorefractive effect.

Average Intensities with No Applied E Field	
Shuttered beam with no interaction	.1114 ± .0001 V
Shuttered beam with interaction	.1100 ± .0001 V
Non-Shuttered beam with no interaction	.2224 ± .0002 V
Non-Shuttered beam with interaction	.2202 ± .0002 V

Average Intensities with Applied E Field	
Shuttered beam with no interaction	.1105 ± .0001 V
Shuttered beam with interaction	.1083 ± .0001 V
Non-Shuttered beam with no interaction	.2412 ± .0002 V
Non-Shuttered beam with interaction	.2377 ± .0002 V

A. 2-Beam Coupling

An effect highly resembling The Photorefractive Effect was very clearly observed. This can easily be seen in Fig. 8 and Fig. 9. where the blue line is the shuttered beam and the red is the line which simply passes through the crystal. One other thing that is important to note is that the effect takes less than a second to respond meaning that this particular crystal has very mobile charge carriers. The measured averages for the intensities of the beam can be found in Table I.

B. 4-Wave Mixing

When the 4-Wave Mixing technique was first used with no applied field we got data much like that of Fig. **??**

When all the other stray beams were tested, simmilar static was produced. Next, this experiment was repeated in the applied electric field of 5000V and resulted in Fig. **??**

Again, this Brownian motion-like static was obtained where the measured voltage never wanders more than a hundredth of a volt away from its starting place.

V. ANALYSIS

A. 2-Beam Coupling

Although no ultimate calculation was obtained, we will go through the steps that would have been taken if we had all of the data required.

We made the assumption that $n_e \approx n_0 \approx n \approx 2.554$. Next we must find $\tilde{\theta}$ which was calculated from Snell's law via

$$\sin\tilde{\theta} = \frac{n_1}{n_2}\sin\theta \approx \frac{1}{n_2}\sin\theta = \frac{1}{2.55}\sin 14 = .0947 \pm .0194. \quad (18)$$

So then we obtain

$$\tilde{\theta} = \arcsin .0947 = .0948 \pm .0194. \quad (19)$$

Calculate the gain factors for the different polarizations $\tilde{\Gamma^p}$ and $\tilde{\Gamma^s}$. This is the last calculation that we can do towards getting r_{eff}.

$$\tilde{\Gamma}^s = \frac{1}{\tilde{d}}\ln\left[\frac{I_{1_s}}{I_{2_s}}\frac{I_{2_{0_s}}}{I_{1_{0_s}}}\right]; \quad \tilde{\Gamma}^p = \frac{1}{\tilde{d}}\ln\left[\frac{I_{1_p}}{I_{2_p}}\frac{I_{2_{0_p}}}{I_{1_{0_p}}}\right]. \quad (20)$$

Where the different I's correspond the the intensities when tested with the 2 different polarization. $I_{1_{0_p}}$ and $I_{2_{0_p}}$ are the intensities of the beams when they individually enter the crystal (no coupling). We forgot to take our data at 2 different polarizations so cannot calculate any further as the lab manual instructs.

We will continue our calculation so that we might find another parameter to compare our data to. We calculate the effective thickness of the crystal $\tilde{d}$ and the interface grating Λ.

$$\tilde{d} = \frac{d}{\cos\tilde{\theta}} = \frac{10^7}{\cos(\arcsin .0947)} = 1.00 \pm .1 \times 10^7 \text{nm} \quad (21)$$

and

$$\Lambda = \frac{\lambda}{2n\sin\tilde{\theta}} = \frac{638.2nm}{2 \times 2.55 \times .0947} = 1,284 \pm 690nm. \quad (22)$$

Which quickly leads to both of the E calculations

$$E_d = \frac{2\pi\left(1.3806 \times 10^{-23}\frac{J}{K}\right)(291K)}{(1.6022 \times 10^{-19}C)(1.28 \times 10^{-6}m)} = 1.28 \pm .10 \times 10^5 \frac{V}{m}. \quad (23)$$

Now we calculate $\tilde{\Gamma}$ using the rather large Eqn. 27. Note that since a measurement for r_{eff} could not be obtained a value for it was taken from [3].

$$r_{eff} = 4.35 \pm .01 \times 10^{-12} \quad (24)$$

$$(25)$$

and so we get that

$$\mathcal{C} = \frac{2\pi n^3}{\lambda\cos(\tilde{\theta})} r_{eff} = 7.17 \pm .02 \times 10^{-4}. \quad (26)$$

From the lab manual we obtain

$$\tilde{\Gamma} = \mathcal{C}\frac{E_d(1+E_d/E_q)+E_a^2/E_q}{(1+E_d/E_q)^2+E_a^2/E_q^2}. \quad (27)$$

Next we solve for E_q and E_a where E_q is the maximum value the field can have and E_a is the induced electric field. In order to do this we would need our $\tilde{\Gamma}$ for both the electric field on and the electric field off via

$$\tilde{\Gamma} = -\frac{1}{.01\text{ m}}\ln\left[\frac{I_1}{I_2}\frac{I_{2_0}}{I_{1_0}}\right]. \quad (28)$$

$$\tilde{\Gamma}_{\text{no E}} = -100\ln\left[\frac{.1100}{.2202}\frac{.2224}{.1114}\right] = .270 \pm .183\text{m}^{-1}. \quad (29)$$

$$\tilde{\Gamma}_{\text{with E}} = .549 \pm .174\text{m}^{-1}. \quad (30)$$

Now we may surmise E_a and E_d. For E_a we know that the crystal sat between 2 parallel plates. This means that the electric field across the plates is simply

$$E_a = \frac{V}{d} = \frac{5000}{.005} = 1 \pm .1 \times 10^6\frac{V}{m}. \quad (31)$$

Here we have used the distance half way through the crystal as an approximation of the field everywhere in the crystal. This is also the point where the field ought to be strongest since it is equidistant from both plates.

Now we may calculate ad compare E_q by using this formula. Obviously, $E_a = 0$ when there is no voltage across the crystal so we have from simplifying Eqn. 27 that

$$E_{q\text{ no E}} = \frac{1}{\mathcal{C}/\tilde{\Gamma}_{\text{no E}} - 1/E_d} = 3.78 \pm .24 \times 10^2. \quad (32)$$

Now E_q can be calculated from the data collected from when the voltage was on.

$$E_{q\text{ w/E}} = \frac{-\mathcal{C}\left(E_a^2+E_d^2\right)+2E_d\tilde{\Gamma}_{\text{no E}}}{2\mathcal{C}E_d - 2\tilde{\Gamma}_{\text{no E}}} + \frac{\sqrt{\mathcal{C}^2\left(E_a^2+E_d^2\right)^2 - 4E_a^2\tilde{\Gamma}^2_{\text{no E}}}}{2\mathcal{C}E_d - 2\tilde{\Gamma}_{\text{no E}}} \quad (33)$$

$$= 7.66 \pm .24 \times 10^2. \quad (34)$$

Now let us calculate the number density N_A from both of them. We take from the lab manual that $\epsilon \approx 3400$ and $N_A(1 - N_A/N_D) \approx N_A$. Where N_D is the number of donor impurities. We also have from the lab manual that

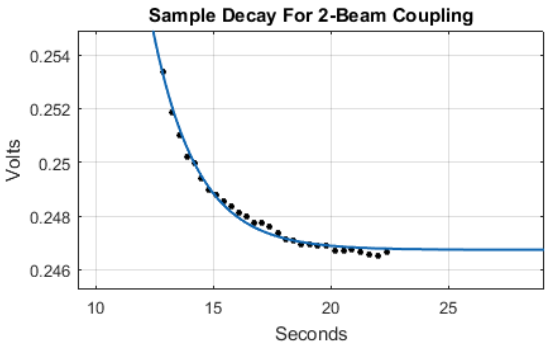

Figure 5: A sample graph of a fit of Eqn. 16 to the data of a single decay of the non-shuttered beam. Many of these were averaged together to get an approximate decay rate from the diffracted beam when both beams are incident on the crystal.

$$E_q = \frac{\Lambda e}{2\pi\epsilon_0\epsilon}N_A(1 - N_A/N_D); \quad (35)$$

$$N_{A\text{ no E}} = \frac{2\pi\left(8.854\times10^{-12}\right)(3400)\left(3.78\times10^2\right)}{(1.264\times10^{-6})(1.602\times10^{-19})} \quad (36)$$

$$= 3.53 \pm .24 \times 10^{20}. \quad (37)$$

$$N_{A\text{ w/E}} = 7.16 \pm .22 \times 10^{20}. \quad (38)$$

In an attempt to make up for the data not taken in the 4-Wave Mixing experiment, data was used from the 2-Beam Coupling experiment to fit Eqn. 16 in an attempt to quantify ν_{decay}. Data was used from the 2-Beam Coupling with no electric field because the decays are larger and easier to find.

We averaged 5 of the clearest decays from Fig. 8 to obtain

$$\eta_0 = .799 \pm .001 \quad (39)$$

and

$$\nu_{decay} = -.529 \pm .055s^{-1}. \quad (40)$$

R^2 values ranged from around .97 to .99 in our fits.

Unfortunately repeating this process for the applied electric field data was impossible because of aliasing.

B. 4-Wave Mixing

Without any well behaved data there was little analysis to be done directly. However, considerable time was put into proving that the data obtains was nothing but noise so that is what will be presented.

Although there was no obvious pattern in the static in Fig. 10 and Fig. 11 a regression was run on it in the unlikely case that a pattern might be found mathematically. The default MATLAB fitting algorithm was used to fit the data to

$$a * \text{sq}\left(\pi\frac{(x+p)}{L}\right) - b. \quad (41)$$

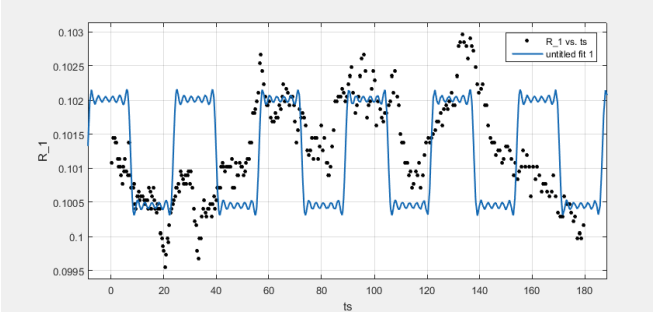

Figure 6: The best fit to the function variable found in Eqn. 41 to the 4-Wave Mixing data found in Fig. 10. If the photorefractive effect was present we would see a high correlation to a square wave because the shutter turned the effect on and off like a switch. Note the lack of any visible correlation.

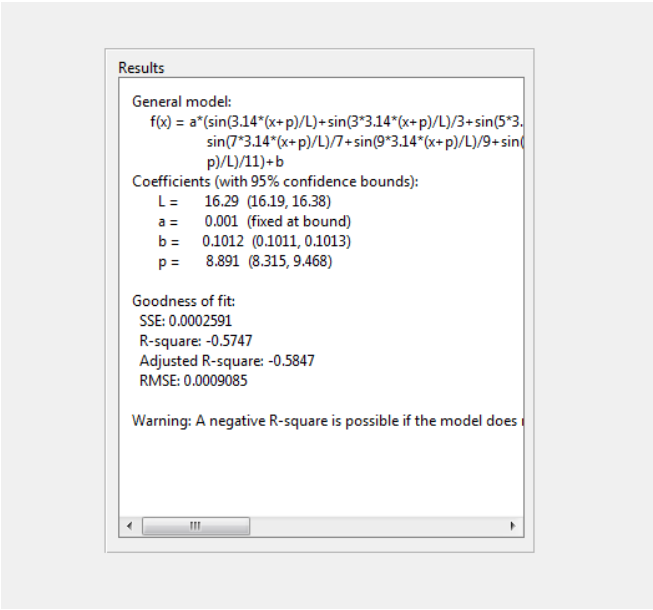

Figure 7: The best fit to the function found in Eqn. 41 to the 4-Wave Mixing data found in Fig. 10. If the photorefractive effect was present we would see a high correlation to a square wave because the shutter turned the effect on and off like a switch. Note the negative R^2 indicating the lack of correlation.

Where the sq(x) is a square wave with period 2π. The fit was done by approximating the square wave with a Fourier series up to 5^{th} order.

It is easy to see that there was no hidden correlation. This technique was repeated to evaluate stray beams with similar results.

VI. CONCLUSION

A. 2-Beam Coupling

Although we were not able to compare our results to the theory in totality, we were able to see very clear troughs and peaks in our graph. This strongly suggests that there was an effect to be measured, despite the fact that very little analysis could be done. Unfortunately a few mistakes along the way kept us from comparing results to theory conclusively.

The normal number density (N_A) for a BSO crystal is about 10^{13}m^{-1} (from [2]) and we calculated a number density to be on the order of 10^{20}m^{-1}.

It would make sense that our crystal has a higher number density than the one tested in [2] since the data was taken in 1995 and the company providing our crystal may have increased the density to increase the induced photoelectric effect. This may also be partially attributed to an overestimation of E_a since the value used was at the strongest point in the field. Other reasons for the lack of predicted results could include a mal-alignment of the beams or the laser heat up time. Although both of these are less likely since they were thoroughly checked.

We cannot conclusively say if the applied electric field increased the mobility of the charge carriers due to aliasing in the applied electric field data. However, simply looking at the graph does imply that the jumps were slightly faster although it is hard to tell because of the small difference between I_0 to I_1.

Despite these rather discouraging results, the value of v_{decay} seemed to fit within expected parameters. According to [4] the decay rates for a BSO crystal can range from 10^{-1} to 10^{-4} s^{-1}. This agrees well with the observed .529 s^{-1}.

It is the opinion of this paper that these results fit previously measured data more than N_A because of the estimation needed for the E_a parameter. If exact data for E_a was obtained then we would likely see results more in agreement with previous measurements.

B. 4-Wave Mixing

We can be sure that the exposure time was not a factor in the failure of the experiment because the effect was observed very quickly in the 2-Beam Coupling. ($\ll$ 15 sec. see Fig. 8) A lot of time was also spent aligning the beams to attempt to eliminate errors from the beams not crossing properly. All of the stray beams were tried and again no effect was observed. We simply found no correlation with the shuttering of the beam.

It is the opinion of this paper that the lack of a response in the 4-wave mixing was due to the difficulty measuring the beams without the chopper. If one looks back to Fig. 3 it is easy to see that the beam that is being measured does not go through the chopper and thus, ambient light could corrupt data.

C. Corrections to 4-Wave Mixing

The attempt to find the correct signal by measuring the chopped beam turned out the same as the regular 4-Wave Mixing with no observed effect. Again, this may have been due to the alignment of the light or not measuring the correct beam, however these are unlikely as they were thoroughly checked.

VII. SUGGESTIONS FOR FURTHER RESEARCH

The main problem that occurred with the 4-Wave Mixing was that the data was not able to be separated from noise. If one looks at Fig. 3 then one will quickly find that the chopped beam is not the one that was measured. Perhaps the experiment could be re-designed so that the chopped beam is directly measured to reduce noise and make it easier to align the beams.

Also, in the future it might be more efficient for experiments to measure v_{decay} as I have with the 2-beam coupling since not many have succeeded in getting the data from the 4-Wave Mixing.

Acknowledgments

I would like to personally acknowledge Dr. John Ruhl and Dr. Jesse Berezovsky for their aid in the setup and execution of the experiment. Thanks go to Nic Vogel and Ryan Chaban for their diligent work in setting up the experiment and their flexibility in working across different classes. Lastly, special thanks to Alex Strang for his exceptional, essential work in coding and implementation of the experiment.
Thanks also to Eric O. Lebgiot, the creator of the uncertainties package for python for his program's help in checking calculations.

[1] John Ruhl, *Study of The Photorefractive Effect* Graduate Lab Non-linear Dymanics Handout (unpublished), and references therein. `http://balin.phys.cwru.edu/SeniorLab/NonLinearOptics?action=AttachFile&do=get&target=NLO_longwriteup.pdf`
[2] G.C. Valley and M.B. Klein, Landmark Papers On Photorefractive Nonlinear Optics **21** (1995).
[3] A. Grunnet-Jepsen, I. Aubrecht, and L. Solymar, Journal Of the Optical Society of America B J. Opt. Soc. Am. B **12**, 921 (1995).
[4] R.A. Mullen and R.W. Hellwarth, J. Appl. Phys. Journal Of Applied Physics **58**, 40 (1985).

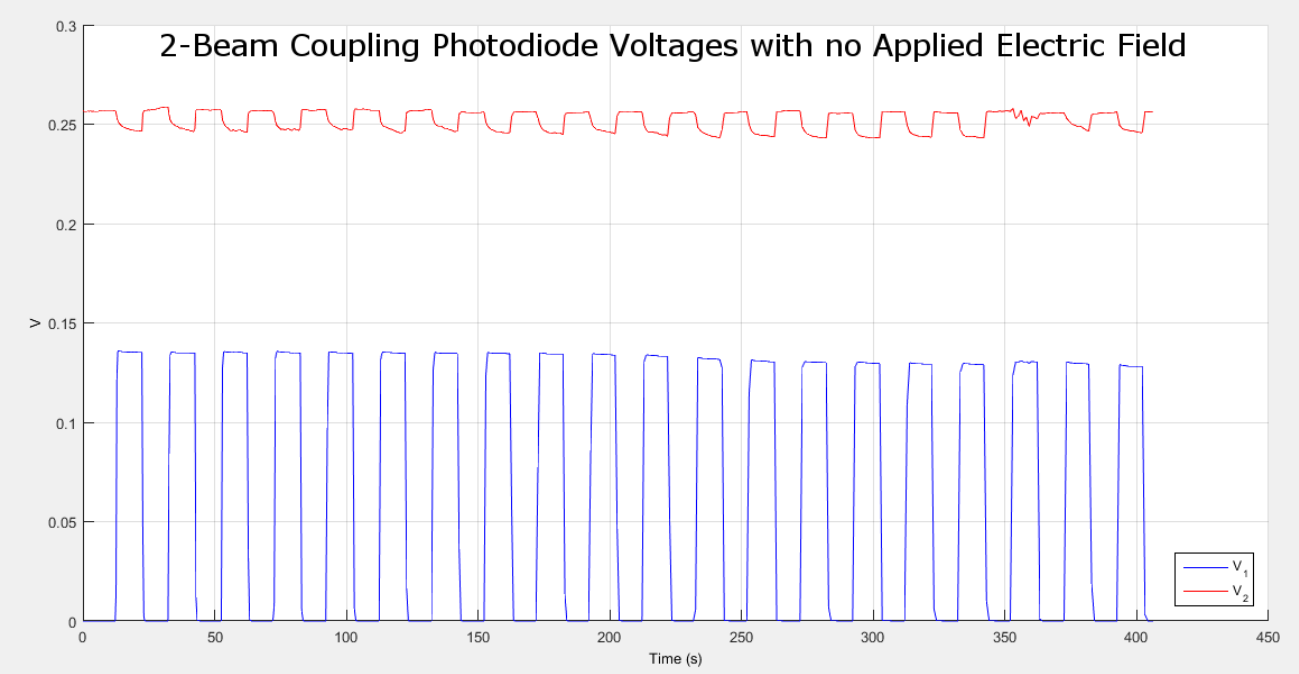

Figure 8: Sample data of photodiode voltages. The beam producing the blue V_1 line is shuttered every 15 seconds (the shuttered beam) while the beam representing the red V_2 line simply passes through the crystal.

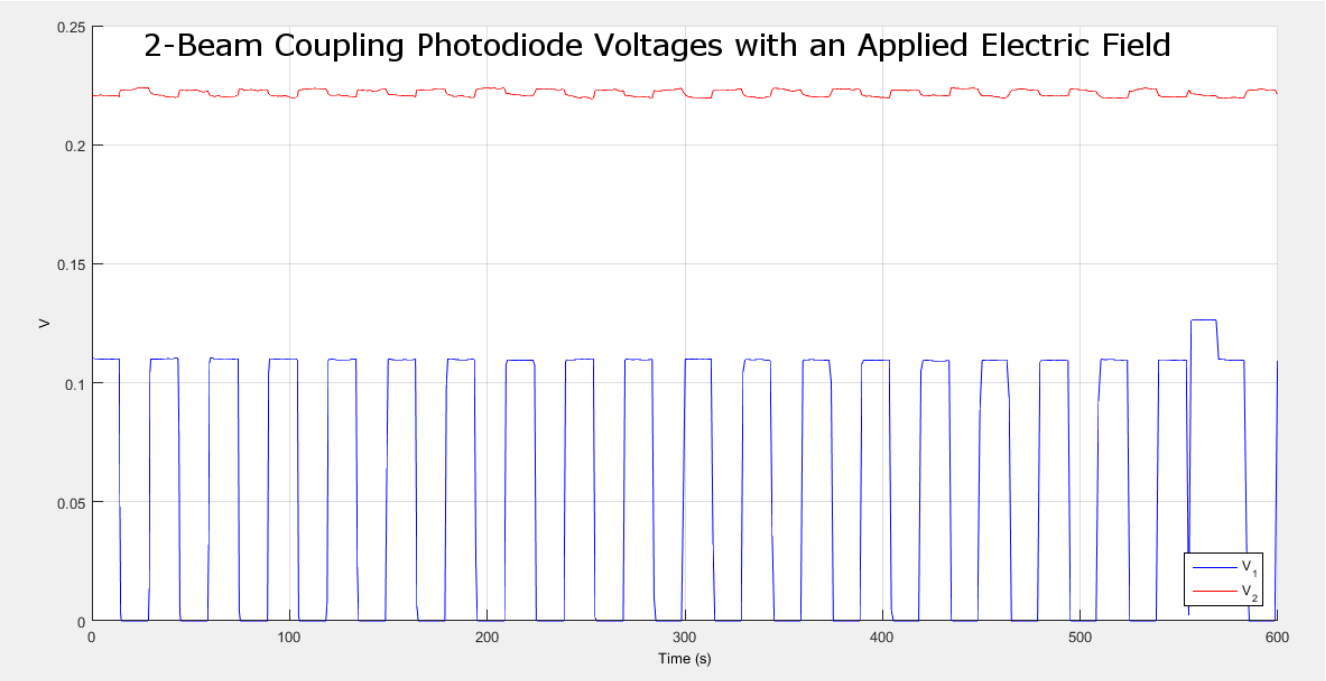

Figure 9: Sample data of photodiode voltages. The beam producing the blue V_1 line is shuttered every 15 seconds (the shuttered beam) while the beam representing the red V_2 line simply passes through the crystal. We can ignore the last, largest hump in the V_2 reading of an induced electric field as it can be accounted for by a shutter malfunction.

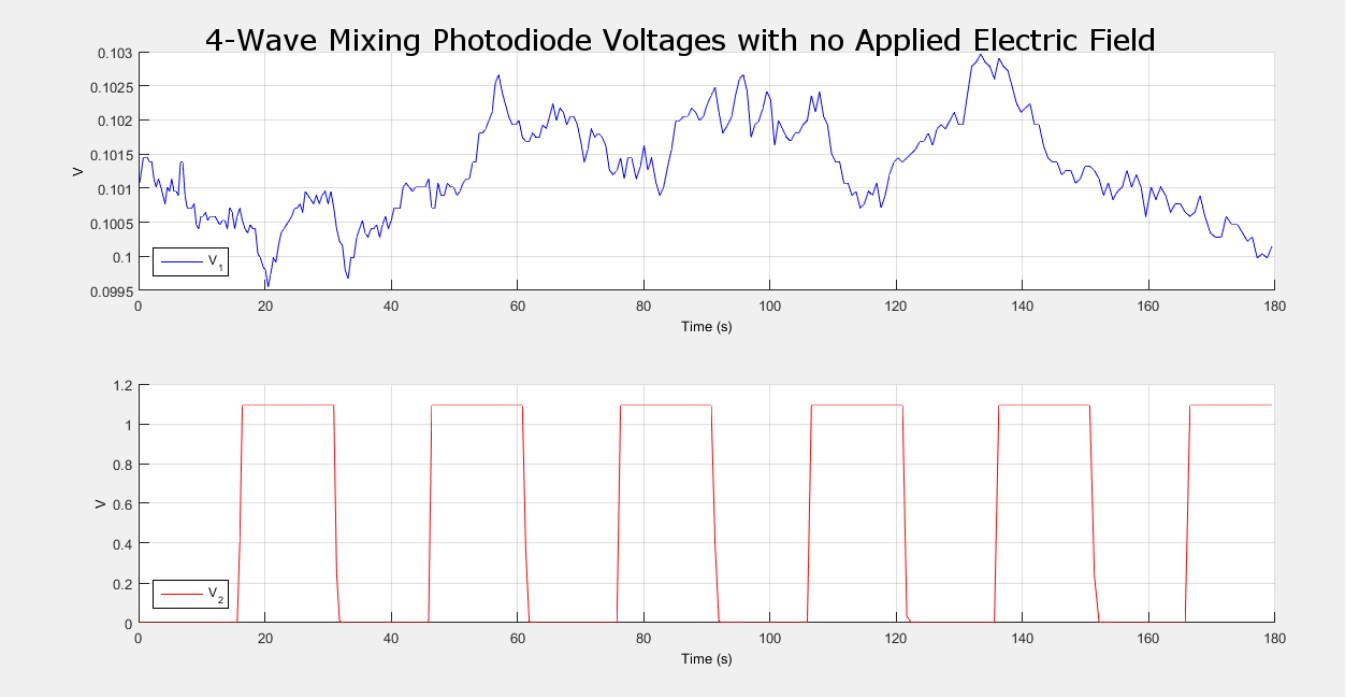

Figure 10: A graph of the static produced when we attempted to measure The Photorefractive Effect using 4-Wave Mixing

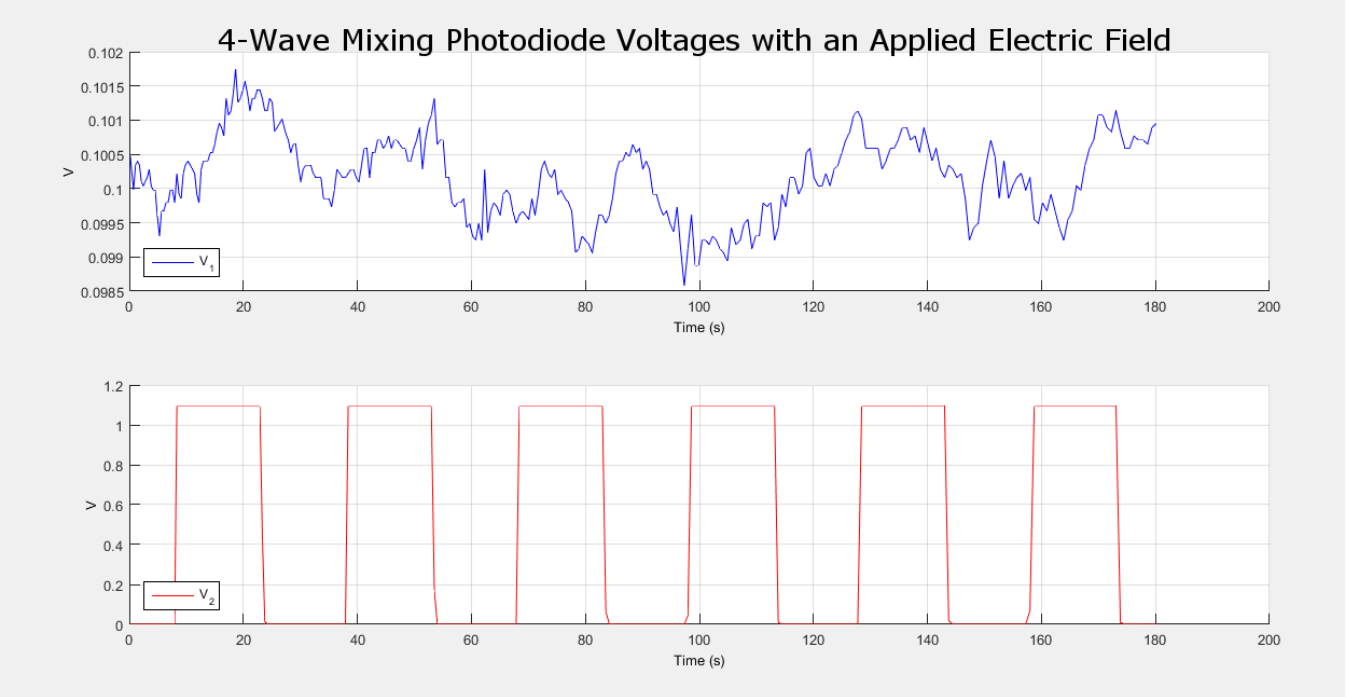

Figure 11: A graph of the static produced when we attempted to measure The Photorefractive Effect using 4-Wave Mixing